Article

Surface Enhanced Raman Spectroscopy based Biosensor with a Microneedle Array for Minimally Invasive In Vivo Glucose Measurements

Jian Ju, Chao-mao Hsieh, Yao Tian, Jian Kang, Ruining Chia, Hao Chang, Yanru Bai, Chenjie Xu, Xiaomeng Wang, and Quan Liu

ACS Sens., **Just Accepted Manuscript** • DOI: 10.1021/acssensors.0c00444 • Publication Date (Web): 19 May 2020

Surface Enhanced Raman Spectroscopy based Biosensor with a Microneedle Array for Minimally Invasive *In Vivo* Glucose Measurements

Jian Ju [a,c], Chao-mao Hsieh[a], Yao Tian [a,d], Jian Kang [a], Ruining Chia [b], Hao Chang [a], Yanru Bai[a], Chenjie Xu [a,e], Xiaomeng Wang[b, f, g, h] and Quan Liu [a,*]

[a] School of Chemical and Biomedical Engineering, Nanyang Technological University, 70 Nanyang Drive, Singapore 637457, Singapore

[b] Lee Kong Chian School of Medicine, Nanyang Technological University, 59 Nanyang Drive, Singapore 636921, Singapore

[c] Department of Chemistry, Oakland University, Rochester, Michigan, United State

[d] Apple South Asia Pte Ltd, 7 Ang Mo Kio Street 64, Singapore 569086, Singapore

[e] Department of Biomedical Engineering, City University of Hong Kong, 83 Tat Chee Avenue, Kowloon, Hong Kong SAR.

[f] Institute of Molecular and Cell Biology, 61 Biopolis Drive, Proteos, Agency for Science Technology & Research, Singapore, 138673

[g] Institute of Ophthalmology, University College London, United Kingdom, EC1V 9EL

[h] Singapore Eye Research Institute, The Academia, 20 College Road Discovery Tower Level 6, Singapore 169856

ABSTRACT: To monitor blood glucose level reliably, diabetic patients usually have to undergo frequent fingerstick tests to draw out fresh blood which is painful and inconvenient with potential risk of cross contamination especially when the lancet is reused or not properly sterilized. This work reports a novel SERS (surface enhanced Raman spectroscopy) sensor for the in situ intradermal detection of glucose based on a low-cost PMMA MN array. After incorporating 1-decanethiol (1-DT) onto the silver-coated array surface, the sensor was calibrated in the range of 0 to 20 mM in skin phantoms then tested for the *in vivo* quantification of glucose in a mouse model of STZ- induced type I diabetes. The results showed that the functional polymethyl methacrylate microneedle (F-PMMA MN) array was able to directly measure glucose in the ISF in a few mins and retain its structural integrity without swelling hydrated. The Clarke error grid analysis of measured data indicated that 93% of the data points lie in zones A and B. Moreover, the MN array exhibited minimal invasiveness to the skin as the skin recovered well without any noticeable adverse reaction in 10 mins after measurements. With further improvement and proper validation, this polymeric MN array based SERS biosensor has the potential to be used in painless glucose monitoring of diabetic patients in the future.

KEYWORDS: *surface enhanced Raman scattering, microneedle array, minimally invasive intradermal measurements, in vivo biosensor, glucose sensing*

Diabetes is a common metabolic disease caused by impaired carbohydrate metabolism. The number of diabetes patients has increased significantly in the past 40 years,[1-3] and the global cost of treating diabetes patients is expected to double by 2030 compared to that in 2015.[4] As an important symptom of diabetes, the blood glucose level is routinely measured for the diagnosis and monitoring of diabetes.[5, 6] Many types of techniques such as colorimetry,[7] electrochemistry,[6] fluorescence, [8] and Raman based methods,[9] have been developed to measure blood glucose levels, most of which require the need of withdraw fresh blood which is painful and inconvenient with potential risk for cross contamination especially when the lancet is reused or not properly sterilized. Recently, intensive research has focused on the development of painless and non-invasive glucose meters to address the above problem. [10, 11] Body fluids such as tear [12]and sweat [13] have drawn much attention because they can be obtained easily without pain. Unlike tear or sweat that are usually ready to be collected with no special device needed, subcutaneous interstitial fluid (ISF) is a thin layer of fluid surrounding cells, which contains glucose, salt, fatty acids, and minerals but requires certain device to collect. Although many studies have revealed that there is a delay in ISF glucose response to changes in blood glucose,[14 15] a consensus has been achieved that the ISF can be considered as the preferred site for a minimally invasive or innovative sensor to conduct subcutaneous glucose monitoring.[16, 17] Methods for ISF measurements may be categorized primarily as electrochemical[18] and optical techniques.[19] Most subcutaneous electrochemical biosensors are based on the principle that glucose is oxidized by glucose oxidase to generate gluconic acid or hydrogen peroxide (H_2O_2).[18] The performance of such enzyme based biosensors

depends on the activity of the enzyme and the amount of dissolved oxygen in the skin biological microenvironment.[20] As the other primary group of noninvasive methods, optical techniques achieve ISF measurements by focusing light into the skin noninvasively.[10] Several studies have reported that subcutaneous measurements can be achieved up to a range of 0.1 to 0.5 mm in depth into tissues *via* mid- or near infrared spectroscopy.[21, 22] However, the recorded spectra can be easily influenced by other non-relevant factors such as dissolved salt, temperature and even pulse and respiration.[21, 22] Raman spectroscopy can detect more specific chemical information and the unique vibrational signatures of target molecules.[23,24] However, the Raman signal of biomolecules is intrinsically weak, which limits the application of Raman spectroscopy in biosensing. Fortunately, surface-enhanced Raman scattering (SERS) effectively overcomes this weakness in many circumstances because it enables dramatic enhancement of Raman signals.[25, 26] SERS has been demonstrated for detection of Raman signals, which was enhanced by silver nanoparticles injected to the proximity of Raman molecules, from a location deeper than 700 μm below the tissue surface, but the subcutaneous injection of metal materials can produce toxicity [27] thus this strategy cannot be applied to human skin. Another strategy for a subcutaneous SERS glucose sensor is to implant a device subcutaneously into the body. Van Duyne et al. developed a quantitative *in vivo* glucose sensor based on SERS for the continuous monitoring of glucose level in a mouse model [28-30] demonstrating the enhanced selectivity and reusability of the sensor. However, the sensor needs to be implanted subcutaneously which involves surgery procedures. Choo et al. reported a Raman sensor for measuring glucose level in the aqueous humor of *ex vivo* rabbit eyes,[31] in which the SERS implant was positioned between the center and the edge of the cornea by a precise surgery. To apply SERS based sensors in a broader range of applications, it is necessary to develop a method that does not require implantation or surgery but still can reach subcutaneous target molecules.

The microneedle can be an excellent candidate for this purpose since microneedles have been increasingly applied to transdermal drug delivery for vaccination as well as the treatment of diabetes, neuralgia and cancer.[32, 33] Due to the short microneedle tip (50 to 900 μm), its penetration through the superficial skin usually does not reach the nerves and blood vessels containing dermis layer, thus enabling painless and blood-free drug delivery.[34-37] Microneedles have been also applied to the detection of clinically relevant biomarkers such as glucose,[38, 39] lactate, [40, 41] alcohol, [42] and metal ion[43], *etc.* More recently, Van Duyne et al. reported the development of a SERS sensor with a plasmonic microneedle array coated with gold nanorods as a minimally invasive platform for pH sensing in *ex vivo* human skin.[44] For glucose measurements, microneedles with a porous structure or a hollow core have been typically used as a skin-pricking device for the collection of glucose in ISF and actual measurements were performed slightly later outside the skin rather than in situ.[45, 46] The potential issues with this strategy include needle tip fracture, elevated contamination risk, and loss of extracted body fluids, etc. To address these issues, the direct measurements of glucose signals from microneedle tips in situ would be most desirable. Our group has previously reported that a stainless steel microneedle coated by silver can be used to directly measure SERS signals from glucose for decent glucose level estimation in skin phantoms.[47] Then we showed that a hollow agarose needle could be used to achieve the same goal to significantly save needle cost with slightly compromised estimation accuracy.[48] However, the past microneedle research for direct intradermal measurements has the following issues: first, no *in vivo* efficacy has been demonstrated; second, the stainless steel microneedle is costly and can easily cause permanent skin damages while there are no established protocols for fabricating solid agarose microneedle arrays yet. As a commercially available alternative, polymer such as polymethyl methacrylate (PMMA) made microneedles can serve as an intermediate candidate because such microneedle arrays are cheap with sufficient mechanical strength but do not easily scratch skin. Moreover, certain polymer materials possess high light transmittance[49] and are biocompatible materials[50] thus suitable for direct *in vivo* intradermal measurements through microneedles.

This article describes a novel SERS glucose sensor based on a PMMA microneedle (PMMA MN) array for direct in situ intradermal measurements. This represents an important step towards minimally invasive, painless, low-cost *in vivo* glucose measurements without the need of blood drawing. Polymer materials PMMA with high light transmittance is employed to prepare the microneedles array. [49] Then, the PMMA MN array was coated with silver nanoparticles (Ag NPs) to enable surface enhancement of Raman signals. After modified with the glucose capture agent of 1-decanethiol (1-DT), the functional microneedle array was demonstrated to be able to achieve *in vivo* intradermal measurements of glucose from interstitial fluid in a mouse model of STZ- induced type I diabetes. This novel SERS sensor based on the functional PMMA MN array possesses the following five significant properties to achieve *in vivo* intradermal measurements: (1) the PMMA MN array has sufficient mechanical strength to penetrate the skin of mice, which can maintain the needle morphology while dwelling in the skin. (2) The high light transmission of PMMA enables laser light and Raman signals to transmit through the microneedle. (3) Silver nanoparticles coated on the outer wall of the microneedle with poly-dopamine as the anchor to immobilize silver nanoparticles give rise to good surface enhancement. (4) The glucose capturing agent 1-DT attached onto the PMMA MN array improves the enrichment of glucose at the tip of the microneedles in ISF. (5) The array of imprints created by the MN array can recover well in 10 mins without any noticeable adverse reaction. With further improvement and proper validation, this polymeric MN array based SERS biosensor has the potential to be used in painless glucose monitoring of diabetic patients in the future.

■ MATERIALS AND METHODS

Reagents

Silver nitrate ($AgNO_3$) and sodium hydroxide pellets were purchased from Merck (Darmstadt, Germany). D-Glucose, 1-decanethiol (1-DT), and 28% ammonium hydroxide (NH_4OH) were ordered from Alfa Aesar (Ward Hill, Massachusetts, USA). Agarose powder was purchased from Vivantis (Selangor, Malaysia). Rhodamine 6G (R6G), dopamine, Streptozocin (STZ), ethanol (purity ≥ 99.5%) were obtained from Sigma Aldrich (St. Louis, Missouri, USA). The PMMA MN arrays were purchased from Micropoint Technologies (Pioneer Junction, Singapore). Nanopure water (18.3 MΩ · cm) was used throughout the experiments. All chemicals used were of the analytical grade. A microwave oven (Sharp, Osaka, Japan) was used to prepare agarose gels.

Fabrication of Ag-Coated PMMA Microneedle Array

The PMMA MN array with required light transmission and mechanical strength was prepared *via* a simple micro-molding

method. Briefly, a PMMA MN array was obtained by pouring PMMA solution into a custom-designed stainless steel master-mold (Micropoint Technologies, Singapore), then going through the steps of degassing and curing. The resulting pyramidal microneedle was a 10 × 10 array each with a side length of 200 μm in the square base and a height of 500 μm. The raw PMMA MN array was washed with ethanol and DI water then dried in the vacuum oven at 40 ℃ after which the following steps will be conducted. First, an agarose gel layer was formed on the back surface of the PMMA MN to protect the MN back surface from subsequent treatment in order to preserve the high light transmission property of this surface. A 5% agarose solution was boiled in the microwave oven and cooled down to 60°C. Then the PMMA MN array was carefully placed on the agarose gel with tweezers to protect its back. Second, the protected PMMA MN was moved into 10-mL dopamine (1.2 mM) in tris-HCl (pH = 8.5) solution and immersed in for 24 h. The change of the solution from colorless to dark brown in color implied that the dopamine has been self-polymerized into poly dopamine. Third, the PMMA MN array was coated by Ag NPs using Tollen's method.[48] The poly dopamine wrapped PMMA MN array went through the first step again to protect its back by agarose. Then the PMMA MN array was settled to the bottom of the breaker and the MN tip was ensured to face upward. After that, 1.5-mL $AgNO_3$ at a concentration of 0.03 M and 0.75-mL NaOH at a concentration of 2.5 M was added to the breaker. A total of 0.2-mL NH_4OH was subsequently introduced into the foresaid solution to re-dissolve the precipitates, and then 4.5-mL glucose solution at a concentration of 0.1 M was added. [47, 48] After reaction for 15 mins, the PMMA MN array was taken out using tweezers and placed in deionized water to undergo ultrasonic treatment for 5 sec. The ultrasonic treatment was repeated several times as necessary until the microneedle's surface was clean by visual observation.

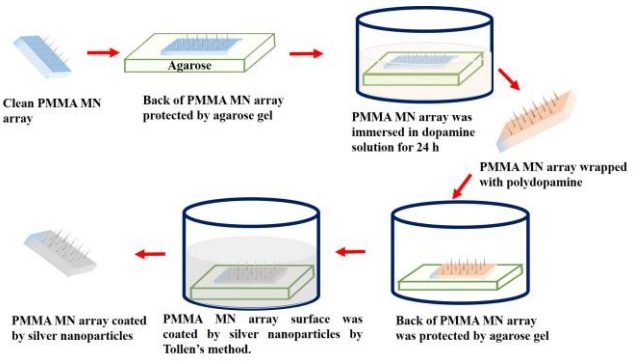

Figure 1. Fabrication process of the Ag-coated PMMA MN array.

Functionalized PMMA MN array for the SERS

For glucose measurements, 1-DT was used as an agent on the PMMA MN array surface to capture glucose molecules nearby. For this purpose, the PMMA MN array was soaked in 1-mM 1-DT ethanol solution for 12 h. In this process, the back of the PMMA MN array was protected by the agarose gel from 1-DT treatment. The resulting functional PMMA MN array was named as the F-PMMA MN array after drying in a vacuum oven.

Preparation of skin phantoms

The skin phantoms were prepared according to our previous work.[48] Briefly, 5% (by mass fraction) agarose solution in water with a total volume of 10 mL was boiled in the microwave oven. The test target molecules, i.e. R6G or glucose, were introduced into the agarose gel after it was cooled down to 60℃ to create the stock phantoms with the test molecules at a series of concentrations. Then the skin phantom of a desired thickness was fabricated by filling the stock phantom (while still in the fluid form) in a well between two glass slides spaced by multiple cover slips. In this study, four cover slips were used to create a skin phantom with a thickness of 1200 μm. The prepared skin phantom was stored in a petri dish after the gel set. It should be noted that the skin phantom was designed to evaluate the F-PMMA MN array in the detection of target molecules for a range of depths in the animal skin. Therefore, it was important to create skin phantoms with an appropriate thickness but not to mimic all optical properties of the skin.

Raman Measurements

We characterized the SERS performance of F-PMMA MN array in the skin phantoms or the animal skin using a portable Raman microspectroscopy system (InnoRam-785S, B&W Tek, Newark, Delaware, USA) coupled to a video microscope accessory (BAC151A, B&W Tek, Newark, Delaware USA. The F-PMMA MN array penetrated the skin phantom or a mouse´s skin to create a passage for laser illumination and Raman detection. A microscope objective (20×, NA = 0.4, Leica, Solms, Germany) was employed to focus 785-nm laser light onto a tip of the F-PMMA MN array. The laser power out of the microneedle tip was around 16.5 mW. The system was adjusted to maximize the detected SERS signal intensity. Raw data were baseline corrected and fluorescence background was removed to yield the spectra shown in subsequent figures.

In vivo detection of the level of glucose in a mouse model of STZ-induced type I diabetes

The C57BL/6 mice were purchased from InVivo Co., Ltd., Singapore. All animal experiments were performed in compliance with the guideline of the ARF-SBS/NIE Nanyang Technological University Institutional Animal Care and Use Committee under the protocol ARF-SBS/ NIE-A0356. To increase the blood glucose level, mice were fed with high-fat and high-sugar diets, and 30 mg/Kg of STZ (Streptozotocin) was injected to destroy part of β cells. In the experiment, the F-PMMA MN array was gently pressed onto the dorsal skin of the mouse. After 15 min, the Raman microspectroscopy system was used to focus laser light onto the mouse skin and detect the SERS signal through a single needle tip of the F-PMMA MN array one at a time. To obtain reference values in the glucose level to compare to results estimated from the SERS signals, OneTouch Ultra glucometer (LifeScan Europe, UK) was utilized to measure the blood glucose level from the tail vein of the mice immediately before the SERS measurements.

■ RESULTS AND DISCUSSION

Characterization of PMMA MN array with and without silver coating

Figure 2 shows the photographs of the PMMA MN array with or without silver coating. As shown in **Figure 2a**, the PMMA MN array without coating appears reasonably transparent. **Figure 2b** shows the back surface of a single needle in the PMMA MN array. The square base can be clearly

found and indicated the pyramidal structure of the PMMA MN array. **Figure 2c** shows a PMMA MN array uniformly coated with Ag NPs. **Figure 2d** shows the side view of a single needle with silver coating. The back surface of a single needle is shown in **Figure 2e**, in which the middle region transmits rather than reflects light thus appearing dark. This implies the formation of Ag NPs on the outer wall of the needle. **Figure 2f** shows the tip of a single needle on focus while the base is out of focus.

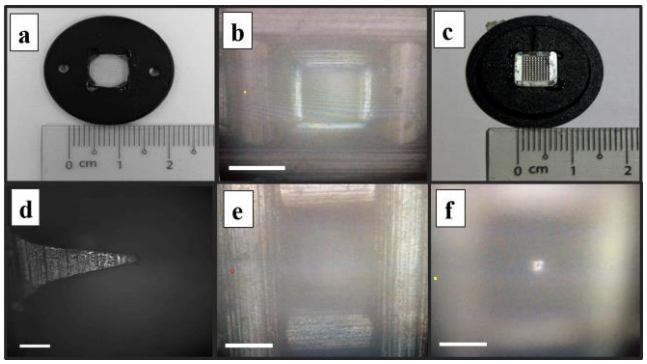

Figure 2. (a) Photograph of the PMMA MN array with no silver coating shown in the centre of the holder. (b) Back surface of a single needle in the PMMA MN array with no silver coating. (c) Photograph of the PMMA MN array coated with silver nanoparticles. (d) Side view of a single needle with silver coating. (e) Back surface and (f) tip of a single needle. The scale bars in (a) and (d-f) indicate 100 μm.

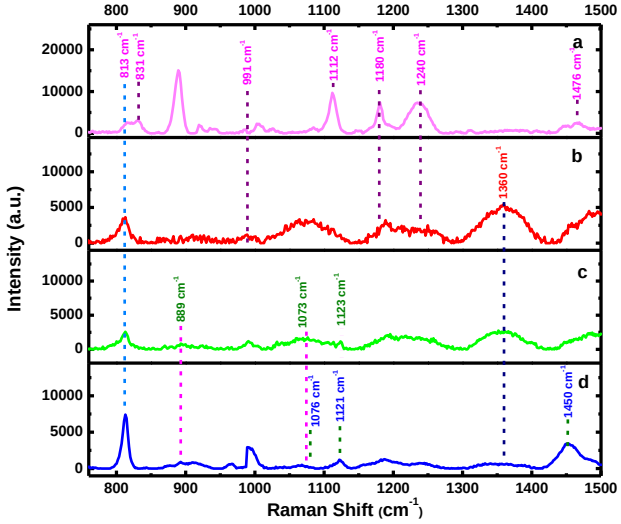

Figure 3. Representative SERS spectra of the original PMMA MN array (line a), the PMMA MN array coated with Ag NPs (line b), 1-DT-modified on the PMMA MN array (line c), i.e. the F-PMMA MN array, and F-PMMA MN array penetrated the skin phantom containing 10-mM Glucose (line d), respectively. The exposure time is always 5000 ms.

Raman spectra confirm the successful surface functionalization of the PMMA MN array. As shown in **Figure 3 (line a)**, the Raman spectrum of the pristine PMMA MN array shows the characteristic bands of PMMA such as those at 813 cm^{-1}, 831 cm^{-1}, 999 cm^{-1}, 1112 cm^{-1}, 1180 cm^{-1}, 1240 cm^{-1} and 1476 cm^{-1}, which can be assigned to, ν(C-O-C), $\nu(CH_2)$, O-CH_3 rock, *ν* (C-C) stretching, *ν* (C-O-C), *ν* (C-O) stretching and (O-CH_3) bending, respectively.[51-54] Poly-dopamine serves as the anchor for the immobilized silver nanoparticles on the PMMA MN array. After dopamine is self-polymerized on the PMMA MN array surface, two prominent broad characteristic bands at 1360 cm^{-1}, which are attributed to the deformation of the catechol group in poly-dopamine molecules.[55] The decreased intensity values of the PMMA bands indicate the successful coating of poly-dopamine and silver nanoparticles as shown in **Figure 3 (line b).** The Raman spectrum of the functional PMMA MN array on which the glucose capturing agent, 1-DT, has modified silver coating clearly shows peaks at 889 cm^{-1}, 1073 cm^{-1} , and 1123 cm^{-1} as in **Figure 3 (line c)**, which are attributed to the 1-DT layer.[9, 48] The characteristic Raman peaks of glucose are located at 1076 cm^{-1} (C-C stretching) and 1121 cm^{-1} (C-O-H deformation) and 1450 cm^{-1} (C-H deformation) as shown in **Figure 3 (line d).**[9, 56] The minor peak shift is due to the binding of the 1-DT on the silver substrate.

Optimization of protocol for coating silver on the PMMA MN array surface

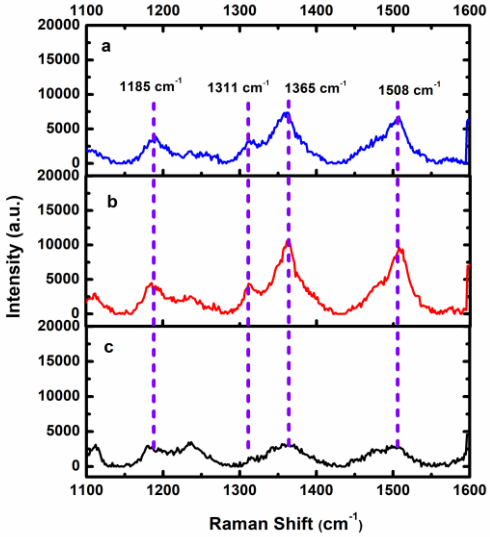

Figure 4. SERS spectra of R6G (10 μM) adsorbed on the needle tips of the F-PMMA MN arrays covered with silver layers of different thicknesses created by the silver sources with a range of concentrations including (a) 0.01-M, (b) 0.03-M, and (c) 0.05-M $AgNO_3$, excited by a laser at 785 nm with a power of 16.5 mW out of the needle tip and an exposure time of 10000 ms.

To find the balance between the SERS enhancement and light transmission through the PMMA MN array tip as a probe for SERS measurements, we optimized the protocol of coating Ag NPs on the PMMA MN array using Tollen´s method. Briefly, we varied the concentration of $AgNO_3$ (0.01, 0.03, and 0.05 M) to create a range of silver layer thicknesses when coating the surface of the PMMA MN array then compared the SERS performance of R6G using the PMMA MN array with different silver layer thicknesses. The F-PMMA MN array penetrated the skin phantom containing 10-μM R6G and the SERS spectra were collected from a needle tip through the back of the PMMA MN array. **Figure 4** shows the measured SERS spectra of R6G (10 μM) in the cases of 0.01-M, 0.03-M and 0.05-M $AgNO_3$ from top

to bottom. Most prominent Raman peaks can be observed in every spectrum, such as those at 1185 cm^{-1}, 1311/1365 cm^{-1} and 1508 cm^{-1}, which can be assigned, C─O─C retching, C─C/C─N stretching and aromatic C─C stretching, [9, 57] respectively. Moreover, the SERS intensity increases when the concentration of the silver source was raised from 0.01 M shown in **Figure 4a** to 0.03 M as shown in **Figure 4b.** After that, the SERS intensity starts to drop as shown in **Figure 4c** when the concentration of the silver source increases further to 0.05 M. This indicates that the permeability of the needle tip is reduced, which causes a decrease in light transmission and in turn the drop in the SERS intensity. This result clearly shows that the silver-coated PMMA MN array can be used to detect Raman probe molecules in a skin phantom, and the thickness of the silver layer on the PMMA MN array plays an important role in the detection of SERS signals. As a result, 0.03-M $AgNO_3$ was used subsequently in this study.

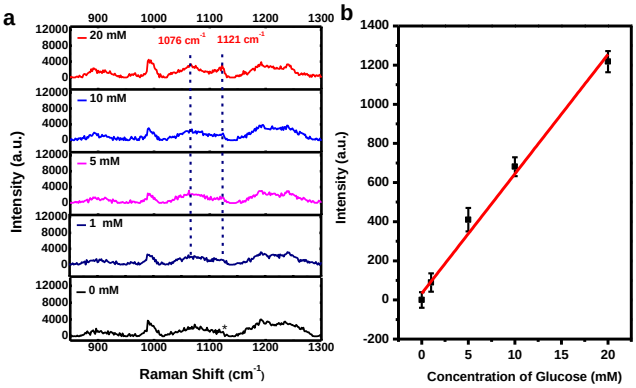

Figure 5. (a) Representative SERS spectra measured from aqueous glucose solutions at a range of concentrations (0, 1, 5, 10 and 20 mM) using the 1-DT (1 mM) modified PMMA MN array coated by AgNPs. **(b)** SERS intensity at the peak of 1121 cm^{-1} as a function of glucose concentration in a range of 0 to 20 mM. The spectra were measured with an excitation power of 16.5 mW out of the needle tip at 785 nm and an exposure time of 10000 ms.

Then the PMMA MN array was modified with the glucose capturing agent, 1-DT, and tested for measuring the glucose level. **Figure 5** demonstrates the SERS spectra measured from the skin phantoms that contained glucose at a range of concentrations (0 to 20 mM). In every dataset, the contribution of 1-DT to the SERS spectrum, measured when the needle has not been used for glucose measurements, was subtracted off to yield the true characteristic glucose Raman peak. **Figure 5a** clearly shows the Raman peaks at 889, 1073 and 1123 cm^{-1} that are attributed to 1-DT[48, 58] and the Raman peaks of the characteristic glucose at 1076 cm^{-1} (C-C stretching) and 1121 cm^{-1} (C-O-H deformation) as shown in Figure 5 b.[9, 48] It should be noted that the spectral increment of SERS spectra detected in this experiment was 1.7 cm^{-1}. **Figure 5b** gives the calibration curve for the F-PMMA MN array. The SERS peak intensity as a function of glucose concentration with a range from 0 to 20 mM is $\boldsymbol{I} = 46.64 \times \boldsymbol{C}_{glucose} + 60.13$ ($R = 0.996$) in a linear equation, in which I represents the average intensity of the glucose SERS readings at 1120.3 ± 1.7 cm^{-1} and $\boldsymbol{C}_{glucose}$ represents glucose concentration. Every sample was measured five times using the same microneedle.

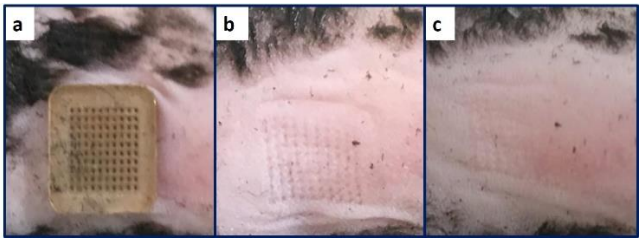

Figure 6. *In vivo* evaluation of the F-PMMA MN array for glucose measurements in the mouse model. **(a)** Photograph of the F-PMMA MN array pressed onto the skin on the back of the mouse. Photograph of the mouse skin **(b)** 5 mins and **(c)** 10 mins after the F-PMMA MN array was taken away.

Afterward, we investigated the *in vivo* performance of the F-PMMA MN array with the mouse model of STZ-induced type I diabetes. The F-PMMA MN array was pressed onto the skin of the mouse's back as seen in **Figure 6a.** The skin photos 5 mins and 10 mins after taking away the array are given in **Figure 6b** and 6**c**. After the removal of F-PMMA MN array, there is an array of imprints due to micro indentation on the mice skin, but no bleeding spots were found as shown in **Figure 6b and 6c**, indicating that the needle tips of F-PMMA MN array penetrated shallow and did not reach the dermis rich in blood vessels and nerve endings.[36] These imprints were almost to completely disappeared in 10 mins after the removal of the array as shown in **Figure 6c**. This fast recovery further confirms that the F-PMMA MN array penetrates only the epidermis of the skin and exhibits minimal invasiveness to the skin. This is important in the clinic applications.

As a feasibility study, we further measured the glucose concentration in the mouse model of STZ- induced type I diabetes. **Figure 7a** shows that the F-PMMA-MN array has been pressed onto the back of the mice near the buttock. This place is easier for the needle tip to penetrate into the skin because the rich muscle in this region serves as a support during pressing. More importantly, the measurement is less affected by the breathing and other body reactions of the mouse as shown in **Video S1.** After the body signs of the anesthetized mouse were stabilized, the mouse was transferred to the stage of the Raman micro spectroscopy system for measurements as in **Figure 7b.** The schematic illustration of glucose measurements using the novel SERS glucose biosensor for *in vivo* transdermal detection is shown in **Figure 7c.** Since the glucose change in ISF lags behind that in blood and the needle tip of the F-PMMA MN array needs time to collect glucose molecules from the ISF, we first optimized the dwelling time of the F-PMMA MN array in the mouse skin as shown in **Figure 7d**. The change in the measured glucose level can start to be seen in 5 mins. But a stable reading is observed after 10 to 15 mins. Therefore, the dwelling time of the array in the mouse skin was set to 15 min in the subsequent measurements. We then measured three mice in the same condition using the array as shown in **Video S2,** and the root-mean-squared error of estimation (RMSE) was calculated to determine the accuracy of the measured glucose levels by comparing with those measured by a commercial glucometer as shown in the equation below and the result is displayed in **Figure 7e.**

$$\mathrm{RMSE} = \sqrt{\frac{1}{N}\sum_{i=1}^{N}(C_{est,i} - C_{ref,i})^2}$$

in which N is the number of data points, C_{est} is the measured glucose concentration and C_{ref} is the corresponding reference glucose concertation. With a total of 15 data points, an RMSE of 1.66 mM is obtained, which is smaller than with our SERS stainless steel microneedle (3.3 mM) [47]and Ag-Coated agarose microneedle (5.1 mM)[48]. A *t*-test was carried out to evaluate the difference in the reading between the SERS sensor and the commercial glucometer and it was found that p-value is 0.938, implying no significant difference. The accuracy of the SERS glucose sensor was then plotted against the reference values from the commercial glucometer using the Clarke error grid. The Clarke error grid is divided into five zones, in which zone A represent clinically correct measurements and lead to proper treatment and zone B contain errors but would not lead to inappropriate treatment. [30] [26] **Figure 7f** gives the Clarke error grid analysis of data from three mice measured at different time points drawn using a commercial software (Matlab R2019b, The MathWorks, Natick, MA, USA). A total of 15 glucose measurements taken by three F-PMMA MN arrays are analyzed using the calibration set obtained earlier by correlating with reference results from the commercial glucometer. As shown in the Clarke error grid, around 93% of the data points lie in zones A and B, with the exception of one data point falling at the edge of the zone D within the hypoglycemic region of the Clarke error grid below 4 mM.[31] This finding suggests that the SERS sensor based on the F-PMMA MN array is promising for future clinical applications especially for diabetes patients.

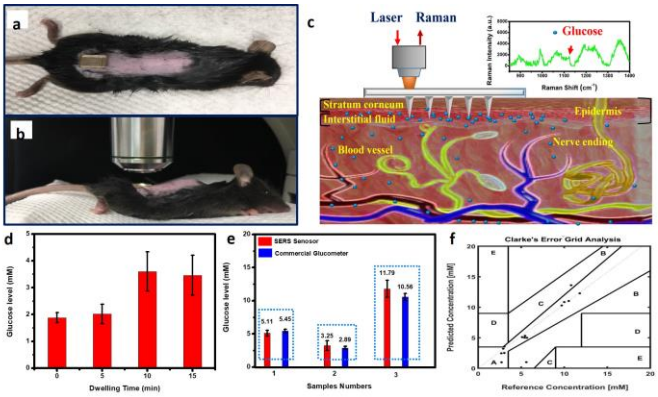

Figure 7. (a) Photograph of the F-PMMA MN array pressed onto the skin on the back of a mouse. (b) Mouse under anesthesia on the stage of the Raman microspectroscopy system for measurements. (c) Schematic illustration of the glucose measurement using the F-PMMA MN array for *in vivo* transdermal detection based on surface enhanced Raman spectroscopy. (d) Glucose level measured using SERS biosensor for a range of dwelling time from 0 to 15 min. (e) Glucose levels measured using our SERS glucose biosens or (red) in comparison with those obtained from a commercial glucometer (blue). We selected three mice with different blood glucose concentrations for testing in which the excitation power was 16.5 mW out of the needle tip at 785 nm and the exposure time was 10000 ms. Each mouse was tested sequentially for 5 times. (f) A Clarke error grid analysis of the *in vivo* glucose measurements using our SERS glucose biosensor in a mouse model of STZ- induced type I diabetes.

■ CONCLUSION

In this work, we developed a novel SERS sensor for the *in vivo* intradermal detection of glucose based on a PMMA MN array. After incorporating 1-DT onto the silver-coated array surface, the sensor was calibrated in the range (0-20 mM) in skin phantoms then tested for the *in vivo* quantification of glucose in a mouse model of STZ- induced type I diabetes. The results showed that the F-PMMA MN array was able to directly measure glucose in the ISF in a few minutes while retaining its structural integrity without swelling. The Clarke error grid analysis of measured data indicated that 93% of the data points lie in zones A and B. Moreover, the MN array exhibited minimal invasiveness to the skin as the skin recovered well without any noticeable adverse reaction in 10 mins after measurements. With further improvement and proper validation, this polymeric MN array based SERS biosensor has the potential to be used in painless glucose monitoring of diabetic patients in the future. In addition, such easily available functional MN demonstrates a significant step forward in the development of portable Raman devices for daily use.

■ ASSOCIATED CONTENT

Supporting Information

The F-PMMA MN array was pressed onto the skin on the back of a mouse (Video S1) and SERS spectra of glucose were detected *in vivo* (Video S2).

■ AUTHOR INFORMATION

Corresponding Author

E-mail address: quanliu@ntu.edu.sg (Q. Liu).

■ ACKNOWLEDGMENTS

Q. Liu acknowledges the funding support from the Ministry of Education in Singapore under its Tier 2 grants (No. MOE2015-T2-2-112 and MOE2017-T2-2-057) and Tier 1 grant (RG129/19), Agency for Science, technology and Research (A*STAR) under its Industry Alignment Fund (Pre-Positioning) (Grant No. H17/01/a0/008 and H17/01/a0/0F9) and KK Women's And Children's Hospital (KKHHF/2018/09).

C.J. Xu acknowledges the funding support from Singapore Agency for Science, Technology and Research (A*STAR) Science and Engineering Research Council Additive Manufacturing for Biological Materials (AMBM) program (A18A8b0059), and internal grant from City University of Hong Kong (#9610472).

X.M. Wang acknowledges the finding support from National Medical Research Council Singapore Large Collaborative Grant DYNAMO (to XW NMRC/OFLCG/001/2017) and National Medical Research Council Singapore Large Collaborative Grant TAAP (to XW NMRC/OFLCG/004/2018)

■ CONFLICTS OF INTEREST

The authors have no conflicts of interest to report.

■ REFERENCES

(1) Yonzon, C. R.; Lyandres, O.; Shah, N. C.; Dieringer, J. A.; Van Duyne, R. P., Glucose sensing with surface-enhanced Raman spectroscopy. In *Surface-Enhanced Raman Scattering*, Springer: 2006; pp 367-379.

(2) Stanley, S. A., Diabetes: Peripheral nerve modulation to treat metabolic disease. *Nat. Rev. Endocrinol.* **2018,** *14* (4), 193.

(3) Collaboration, N. R. F., Worldwide trends in diabetes since 1980: a pooled analysis of 751 population-based studies with 4· 4 million participants. *Lancet* **2016,** *387* (10027), 1513-1530.

(4) Bommer, C.; Sagalova, V.; Heesemann, E.; Manne-Goehler, J.; Atun, R.; Bärnighausen, T.; Davies, J.; Vollmer, S., Global economic burden of diabetes in adults: projections from 2015 to 2030. *Diabetes Care* **2018,** *41* (5), 963-970.

(5) Veiseh, O.; Tang, B. C.; Whitehead, K. A.; Anderson, D. G.; Langer, R., Managing diabetes with nanomedicine: challenges and opportunities. *Nat. Rev. Drug Discovery* **2015,** *14* (1), 45.

(6) Song, Y.; Lu, X.; Li, Y.; Guo, Q.; Chen, S.; Mao, L.; Hou, H.; Wang, L., Nitrogen-doped carbon nanotubes supported by macroporous carbon as an efficient enzymatic biosensing platform for glucose. *Anal. Chem.* **2015,** *88* (2), 1371-1377.

(7) Peng, X.; Wan, G.; Wu, L.; Zeng, M.; Lin, S.; Wang, G., Peroxidase-like activity of Au@ TiO2 yolk-shell nanostructure and its application for colorimetric detection of H2O2 and glucose. *Sensors Actuators B: Chem.* **2018,** *257*, 166-177.

(8) Liu, Y.; Zhu, J.; Xu, Y.; Qin, Y.; Jiang, D., Boronic acid functionalized aza-Bodipy (azaBDPBA) based fluorescence optodes for the analysis of glucose in whole blood. *ACS Appl. Mater. Interfaces* **2015,** *7* (21), 11141-11145.

(9) Ju, J.; Liu, W.; Perlaki, C. M.; Chen, K.; Feng, C.; Liu, Q., Sustained and cost effective silver substrate for surface enhanced Raman spectroscopy based biosensing. *Sci. rep.* **2017,** *7* (1), 6917.

(10) Delbeck, S.; Vahlsing, T.; Leonhardt, S.; Steiner, G.; Heise, H. M., Non-invasive monitoring of blood glucose using optical methods for skin spectroscopy-opportunities and recent advances. *Anal. Bioanal. Chem.* **2019,** *411* (1), 63-77.

(11) Nawaz, A.; Øhlckers, P.; Sælid, S.; Jacobsen, M.; Akram, M. N., Non-invasive continuous blood glucose measurement techniques. *J.Bioinformatics and Diabetes* **2016,** *1* (3), 01.

(12) Zhang, J.; Hodge, W.; Hutnick, C.; Wang, X., Noninvasive diagnostic devices for diabetes through measuring tear glucose. *J. diabetes Sci. Technol.* **2011,** *5* (1), 166-172.

(13) Lee, H.; Song, C.; Hong, Y. S.; Kim, M. S.; Cho, H. R.; Kang, T.; Shin, K.; Choi, S. H.; Hyeon, T.; Kim, D.-H., Wearable/disposable sweat-based glucose monitoring device with multistage transdermal drug delivery module. *Sci. Adv.* **2017,** *3* (3), e1601314.

(14) Rossetti, P.; Bondia, J.; Vehi, J.; Fanelli, C. G., Estimating plasma glucose from interstitial glucose: the issue of calibration algorithms in commercial continuous glucose monitoring devices. *Sensors (Basel)* **2010,** *10* (12), 10936-52.

(15) Moser, O.; Yardley, J. E.; Bracken, R. M., Interstitial Glucose and Physical Exercise in Type 1 Diabetes: Integrative Physiology, Technology, and the Gap In-Between. *Nutrients* **2018,** *10* (1), 93.

(16) Barrett, C.; Dawson, K.; O'Mahony, C.; O'Riordan, A., Development of Low Cost Rapid Fabrication of Sharp Polymer Microneedles for In Vivo Glucose Biosensing Applications. *ECS J. Solid. State. Sci. Technol.* **2015,** *4* (10), S3053-S3058.

(17) Kolluru, C.; Gupta, R.; Jiang, Q.; Williams, M.; Gholami Derami, H.; Cao, S.; Noel, R. K.; Singamaneni, S.; Prausnitz, M. R., Plasmonic Paper Microneedle Patch for On-Patch Detection of Molecules in Dermal Interstitial Fluid. *ACS Sens* **2019,** *4* (6), 1569-1576.

(18) Bollella, P.; Sharma, S.; Cass, A. E. G.; Tasca, F.; Antiochia, R., Minimally Invasive Glucose Monitoring Using a Highly Porous Gold Microneedles-Based Biosensor: Characterization and Application in Artificial Interstitial Fluid. *Catalysts* **2019,** *9* (7), 580.

(19) Olesberg, J. T.; Coté, G. L.; Cao, C.; Priezzhev, A. V.; Yager, J. R.; Prineas, J. P.; Coretsopoulos, C.; Arnold, M. A.; Olafsen, L. J.; Santilli, M., Optical microsensor for continuous glucose measurements in interstitial fluid. *Proc. of SPIE*. **2006,** *6094*, 609403.

(20) Chinnadayyala, S. R.; Park, K. D.; Cho, S., Editors' Choice—Review—In Vivo and In Vitro Microneedle Based Enzymatic and Non-Enzymatic Continuous Glucose Monitoring Biosensors. *ECS J. Solid. State. Sc.* **2018,** *7* (7), Q3159-Q3171.

(21) Kasahara, R.; Kino, S.; Soyama, S.; Matsuura, Y., Noninvasive glucose monitoring using mid-infrared absorption spectroscopy based on a few wavenumbers. *Biomed. Opt. Express.* **2018,** *9* (1), 289-302.

(22) Heise, H.; Marbach, R.; Koschinsky, T.; Gries, F., Noninvasive blood glucose sensors based on near- infrared spectroscopy. *Artif. Organs* **1994,** *18* (6), 439-447.

(23) Lindquist, N. C.; de Albuquerque, C. D. L.; Sobral-Filho, R. G.; Paci, I.; Brolo, A. G., High-speed imaging of surface-enhanced Raman scattering fluctuations from individual nanoparticles. *Nat. Nanotechnol.* **2019**.

(24) Laing, S.; Jamieson, L. E.; Faulds, K.; Graham, D., Surface-enhanced Raman spectroscopy for in vivo biosensing. *Nat. Rev. Chem.* **2017,** *1* (8).

(25) Sharma, B.; Bugga, P.; Madison, L. R.; Henry, A.-I.; Blaber, M. G.; Greeneltch, N. G.; Chiang, N.; Mrksich, M.; Schatz, G. C.; Van Duyne, R. P., Bisboronic acids for selective, physiologically relevant direct glucose sensing

with surface-enhanced Raman spectroscopy. *J. Am. Chem. Soc.* **2016,** *138* (42), 13952-13959.

(26) Yonzon, C. R.; Haynes, C. L.; Zhang, X.; Walsh, J. T.; Van Duyne, R. P., A glucose biosensor based on surface-enhanced Raman scattering: improved partition layer, temporal stability, reversibility, and resistance to serum protein interference. *Anal. Chem.* **2004,** *76* (1), 78-85.

(27) Asharani, P.; Wu, Y. L.; Gong, Z.; Valiyaveettil, S., Toxicity of silver nanoparticles in zebrafish models. *Nanotechnology* **2008,** *19* (25), 255102.

(28) Yuen, J. M.; Shah, N. C.; Walsh Jr, J. T.; Glucksberg, M. R.; Van Duyne, R. P., Transcutaneous glucose sensing by surface-enhanced spatially offset Raman spectroscopy in a rat model. *Anal. Chem.* **2010,** *82* (20), 8382-8385.

(29) Ma, K.; Yuen, J. M.; Shah, N. C.; Walsh Jr, J. T.; Glucksberg, M. R.; Van Duyne, R. P., In vivo, transcutaneous glucose sensing using surface-enhanced spatially offset Raman spectroscopy: multiple rats, improved hypoglycemic accuracy, low incident power, and continuous monitoring for greater than 17 days. *Anal. Chem.* **2011,** *83* (23), 9146-9152.

(30) Stuart, D. A.; Yuen, J. M.; Shah, N.; Lyandres, O.; Yonzon, C. R.; Glucksberg, M. R.; Walsh, J. T.; Van Duyne, R. P., In vivo glucose measurement by surface-enhanced Raman spectroscopy. *Anal. Chem.* **2006,** *78* (20), 7211-7215.

(31) Yang, D.; Afroosheh, S.; Lee, J. O.; Cho, H.; Kumar, S.; Siddique, R. H.; Narasimhan, V.; Yoon, Y.-Z.; Zayak, A. T.; Choo, H., Glucose sensing using surface-enhanced Raman-mode constraining. *Anal. Chem.* **2018,** *90* (24), 14269-14278.

(32) Chen, W.; Tian, R.; Xu, C.; Yung, B. C.; Wang, G.; Liu, Y.; Ni, Q.; Zhang, F.; Zhou, Z.; Wang, J., Microneedle-array patches loaded with dual mineralized protein/peptide particles for type 2 diabetes therapy. *Nat. Commun.* **2017,** *8* (1), 1777.

(33) Yang, J.; Liu, X.; Fu, Y.; Song, Y., Recent advances of microneedles for biomedical applications: drug delivery and beyond. *Acta. Pharm. Sin. B.* **2019**.

(34) Ventrelli, L.; Marsilio Strambini, L.; Barillaro, G., Microneedles for transdermal biosensing: current picture and future direction. *Adv. healthc. Mater.* **2015,** *4* (17), 2606-2640.

(35) Sullivan, S. P.; Murthy, N.; Prausnitz, M. R., Minimally invasive protein delivery with rapidly dissolving polymer microneedles. *Adv. Mater.* **2008,** *20* (5), 933-938.

(36) Than, A.; Liu, C.; Chang, H.; Duong, P. K.; Cheung, C. M. G.; Xu, C.; Wang, X.; Chen, P., Self-implantable double-layered micro-drug-reservoirs for efficient and controlled ocular drug delivery. *Nat. Commun.* **2018,** *9* (1), 4433.

(37) Kim, M.; Jung, B.; Park, J.-H., Hydrogel swelling as a trigger to release biodegradable polymer microneedles in skin. *Biomaterials* **2012,** *33* (2), 668-678.

(38) Wang, P. M.; Cornwell, M.; Prausnitz, M. R., Minimally invasive extraction of dermal interstitial fluid for glucose monitoring using microneedles. *Diabetes Technol. Ther.* **2005,** *7* (1), 131-141.

(39) El-Laboudi, A.; Oliver, N. S.; Cass, A.; Johnston, D., Use of microneedle array devices for continuous glucose monitoring: a review. *Diabetes Technol. Ther.* **2013,** *15* (1), 101-115.

(40) Bollella, P.; Sharma, S.; Cass, A. E. G.; Antiochia, R., Microneedle-based biosensor for minimally-invasive lactate detection. *Biosens. Bioelectron.* **2019,** *123*, 152-159.

(41) Lee, H.; Choi, T. K.; Lee, Y. B.; Cho, H. R.; Ghaffari, R.; Wang, L.; Choi, H. J.; Chung, T. D.; Lu, N.; Hyeon, T., A graphene-based electrochemical device with thermoresponsive microneedles for diabetes monitoring and therapy. *Nat. Nanotechnol.* **2016,** *11* (6), 566.

(42) Mohan, A. V.; Windmiller, J. R.; Mishra, R. K.; Wang, J., Continuous minimally-invasive alcohol monitoring using microneedle sensor arrays. *Biosens. Bioelectron.* **2017,** *91*, 574-579.

(43) Miller, P. R.; Xiao, X.; Brener, I.; Burckel, D. B.; Narayan, R.; Polsky, R., Microneedle- Based Transdermal Sensor for On- Chip Potentiometric Determination of K+. *Adv. Healthc. Mater.* **2014,** *3* (6), 876-881.

(44) Park, J. E.; Yonet-Tanyeri, N.; Vander Ende, E.; Henry, A.-I.; Perez White, B. E.; Mrksich, M.; Van Duyne, R. P., Plasmonic Microneedle Arrays for in Situ Sensing with Surface-Enhanced Raman Spectroscopy (SERS). *Nano Lett.* **2019,** *19* (10), 6862-6868.

(45) Strambini, L.; Longo, A.; Scarano, S.; Prescimone, T.; Palchetti, I.; Minunni, M.; Giannessi, D.; Barillaro, G., Self-powered microneedle-based biosensors for pain-free high-accuracy measurement of glycaemia in interstitial fluid. *Biosens. Bioelectron.* **2015,** *66*, 162-168.

(46) Miller, P. R.; Narayan, R. J.; Polsky, R., Microneedle-based sensors for medical diagnosis. *J. Mater. Chem. B* **2016,** *4* (8), 1379-1383.

(47) Yuen, C.; Liu, Q., Towards in vivo intradermal surface enhanced Raman scattering (SERS) measurements: silver coated microneedle based SERS probe. *J. Biophotonics* **2014,** *7* (9), 683-689.

(48) Yuen, C.; Liu, Q., Hollow agarose microneedle with silver coating for intradermal surface-enhanced Raman measurements: a skin-mimicking phantom study. *J. Biomed. Opt.* **2015,** *20* (6), 061102.

(49) Chen, S.; Ye, F.; Tang, G.; Wang, X., High Toughness and Light Transmittance of PMMA Composite Prepared via In-Situ Polymerization with Incorporating Self-Assembled Dendritic Gel Networks. *J. Macromol. Sci. A* **2014,** *51* (2), 173-179.

(50) Kim, S. J.; Choi, B.; Kim, K. S.; Bae, W. J.; Hong, S. H.; Lee, J. Y.; Hwang, T.-K.; Kim, S. W., The potential role of polymethyl methacrylate as a new packaging material for the implantable medical device in the bladder. *Biomed. Res. Int.* **2015,** *2015*.

(51) Chen, J.; Li, J.; Xu, L.; Hong, W.; Yang, Y.; Chen, X., The Glass-Transition Temperature of Supported PMMA Thin Films with Hydrogen Bond/Plasmonic Interface. *Polymers* **2019,** *11* (4), 601.

(52) Thomas, K.; Sheeba, M.; Nampoori, V.; Vallabhan, C.; Radhakrishnan, P., Raman spectra of polymethyl methacrylate optical fibres excited by a 532 nm diode pumped solid state laser. *J. opt. A-Pure. Apply. Op.s* **2008,** *10* (5), 055303.

(53) Thakur, V. K.; Vennerberg, D.; Madbouly, S. A.; Kessler, M. R., Bio-inspired green surface functionalization of PMMA for multifunctional capacitors. *RSC Adv.* **2014,** *4* (13), 6677-6684.

(54) Willis, H.; Zichy, V.; Hendra, P., The laser-Raman and infra-red spectra of poly (methyl methacrylate). *Polymer* **1969,** *10*, 737-746.

(55) Thakur, V. K.; Yan, J.; Lin, M.-F.; Zhi, C.; Golberg, D.; Bando, Y.; Sim, R.; Lee, P. S., Novel polymer nanocomposites from bioinspired green aqueous functionalization of BNNTs. *Polym. Chem.* **2012,** *3* (4), 962-969.

(56) Atkins, C. G.; Buckley, K.; Blades, M. W.; Turner, R. F., Raman spectroscopy of blood and blood components. *Appl. Spectmsc.* **2017,** *71* (5), 767-793.

(57) Liu, Y.; Hu, Y.; Zhang, J., Few-layer graphene-encapsulated metal nanoparticles for surface-enhanced Raman spectroscopy. *J. Phys. Chem. C* **2014,** *118* (17), 8993-8998.

(58) Shafer-Peltier, K. E.; Haynes, C. L.; Glucksberg, M. R.; Van Duyne, R. P., Toward a glucose biosensor based on surface-enhanced Raman scattering. *J. Am. Chem. Soc.* **2003,** *125* (2), 588-593.

Video Captions

Video S1 showing the F-PMMA MN array pressed onto the skin on the back of a mouse.

Video S2 showing the SERS spectra of glucose detected *in vivo* using an F-PMMA MN array pressed onto the skin of a mouse.

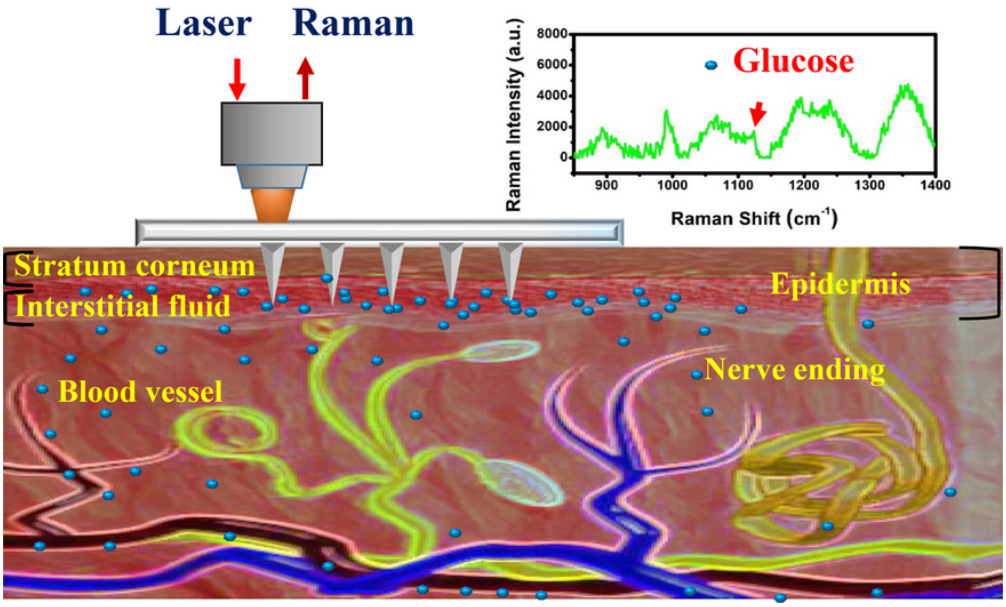

74x44mm (300 x 300 DPI)